Available online at www.sciencedirect.com
SCIENCE DIRECT®
International Journal of Thermal Sciences 45 (2006) 607–614
International Journal of Thermal Sciences
www.elsevier.com/locate/ijts

Conjugate mixed convection transport from a moving vertical plate in a non-Newtonian fluid

Mahesh Kumari [a,*], Girishwar Nath [b]

[a] *Department of Mathematics, Indian Institute of Science, Bangalore 560012, India*
[b] *C/o Dr. S.K. Sinha, KNIT Campus, Type IV/17, KNIT, Sultanpur 228118, India*

Received 26 January 2004; received in revised form 22 June 2005; accepted 22 June 2005

Available online 21 September 2005

Abstract

The conjugate mixed convection–conduction heat transfer of a non-Newtonian power-law fluid on a vertical heated plate which is moving in an ambient fluid has been studied. The system of partial differential equations governing the flow and heat has been solved by using an implicit finite-difference method. The surface heat transfer is found to depend on the non-Newtonian parameter, buoyancy force, generalized Prandtl number, Peclet number and material parameter and it increases with these parameters except for the material parameter where it decreases. The Nusselt number and the wall temperature decrease with increasing distance along the plate. The skin friction coefficient increases with the buoyancy parameter. It also increases with the non-Newtonian parameter near the slot, but decreases away from the slot.

Keywords: Conjugate mixed convection; Moving vertical plate; Non-Newtonian power-law fluids

1. Introduction

The transfer of heat and momentum from a heated moving surface in an otherwise ambient medium occur in many manufacturing processes such as rolling sheet drawn from a die, cooling and/or drying of paper and textile, manufacturing of polymeric sheets, sheet glass and crystalline materials etc. [1,2]. When the material emerges from the die or roller, its temperature is higher than that of the surroundings. Generally, this high temperature is due to the external heating as in the case of hot extrusion. Plastic deformation of the material and the friction between the flowing material and the die also contribute to the heating. In the case of cold extrusion, a portion of heat generated is lost to the die and the remaining heat is dissipated to the environment. In many practical applications, the extruded material passes through a cooling bath as in the case of wire cutting discussed by Fisher [2]. Sakiadis [3] was the first to study the flow due to a solid surface moving with a constant velocity in an otherwise ambient fluid. Due to the entrainment of ambient fluid, this problem represents a different class of boundary layer problem which has a solution different from that of boundary layer flow over a stationary surface. The corresponding heat transfer problem was studied theoretically and experimentally by Tsou et al. [4], theoretically by Erickson et al. [5] and experimentally by Griffin and Thorne [6]. Jeng et al. [7] considered the flow and heat transfer characteristics over a moving surface in an ambient fluid. Moutsoglou and Chen [8] and Takhar et al. [9] examined the effect of buoyancy forces on an inclined surface moving in an ambient fluid.

In the studies mentioned above [3–9], the thickness of the plate was assumed to be small and the plate surface to be isothermal. However, in several practical problems mentioned earlier, the thickness of the emerging plate is finite. When the material loses energy, the temperature distribution in the material becomes important as in the case of continuous casting and plastic extrusion. Jaluria and Singh [10] obtained the temperature distribution for a moving plate and a circular rod for the constant wall temperature case. Chida and Katto [11] analyzed the conjugate heat transfer of continuous moving surface and verified their results by measurement. Karwe and Jaluria [12] have also studied the conjugate heat transfer prob-

* Corresponding author.
E-mail address: mkumari@math.iisc.ernet.in (M. Kumari).

1290-0729/$ – see front matter
doi:10.1016/j.ijthermalsci.2005.06.010

Nomenclature

c_f, c_p	specific heat of the fluid and plate, respectively ..... $J\cdot kg^{-1}\cdot K^{-1}$
C_{fx}	skin friction coefficient, $m(\lvert\partial u/\partial y\rvert)^N_{y=0}/\rho U_0^2$
d	half of the plate thickness ..... m
g	acceleration due to gravity ..... $m\cdot s^{-2}$
Gr_L	Grashof number, $g\beta(T_0 - T_\infty)L^3/(\alpha_f Pr)^2$
K_f, K_p	thermal conductivity of the fluid and plate, respectively ..... $W\cdot m^{-1}\cdot K^{-1}$
L	length scale ..... m
m	consistency index ..... $kg\cdot m^{-1}\cdot s^{N-2}$
N	dimensionless flow index
Nu_x	Nusselt number, $-x(\partial T/\partial y)_{y=0}/(T_w - T_\infty)$
Pe	Peclet number, $U_0 d^2/(\alpha_p L)$
Pr	generalized Prandtl number, $U_0\, L(Re_L)^{-2/(N+1)}/\alpha_f$
R	property (material) parameter, $[(K\rho c)_f/(K\rho c)_p]^{1/2}$
Re_L	Reynolds number defined with respect to L, $U_0^{2-N}\, L^N/(m/\rho)$
Re_x	Reynolds number defined with respect to x, $U_0^{2-N} x^N/(m/\rho)$
Ri_x	Richardson number defined with respect to x, $g\beta(T_0 - T_\infty)x/U_0^2$
T	temperature of the fluid ..... K
T_0	temperature of the plate at the slot ..... K
T_p	temperature of the plate ..... K
T_∞	ambient temperature ..... K
u, v	dimensional velocity components along and normal to the plate ..... $m\cdot s^{-1}$
U_0	velocity of the plate ..... $m\cdot s^{-1}$
U, V	dimensionless velocity components, $U = u/U_0$, $V = (v/U_0)Re_L^{1/(N+1)}$
x, y	dimensional distances along and perpendicular to the plate ..... m
X, Y	dimensionless distances, $X = x/L$, $Y = y\,Re_L^{1/(N+1)}/L$
y_p	dimensional distance within the plate ..... m
Y_p	dimensionless distance, y_p/d

Greek symbols

α	thermal diffusivity ..... $m^2\cdot s^{-1}$
β	coefficient of thermal expansion ..... K^{-1}
θ	dimensionless temperature of the fluid, $(T - T_\infty)/(T_0 - T_\infty)$
θ_p	dimensionless temperature of the plate, $(T_p - T_\infty)/(T_0 - T_\infty)$
λ	buoyancy parameter, $Gr_L/Re_L^{4/(N+1)} = g\beta(T_0 - T_\infty)L/U_0^2$
ρ	density ..... $kg\cdot m^{-3}$

Subscripts

f, p	conditions in the fluid and on the plate, respectively
w, ∞	conditions at the wall and in the ambient fluid, respectively

lem under boundary layer approximations. Further, Karwe and Jaluria [13,14] and Kang and Jaluria [15] considered more general problem and solved both the boundary layer and the Navier–Stokes equations along with the energy equation by using finite-difference technique. In a recent review, Viskanta and Bergman [16] discussed several aspects of the moving plate problem which include the effects of the conjugate boundary conditions at the plate surface, the effects of an externally induced forced flow and the effects of suction and injection through the stretched surface. Al-Sanea and Ali [17] studied the effects of the extrusion die and suction/injection at the moving surface on the skin friction and heat transfer with emphasis on the region close to the extrusion slot using the Navier–Stokes and energy equations. They obtained critical Reynolds numbers to distinguish between the self-similar and non-similar regions. However, the buoyancy effects were not considered. Subsequently, Al-Sanea [18] extended the above analysis [17] to include the effects of buoyancy forces.

In recent years, non-Newtonian fluids find increasing applications in chemical process industries, petroleum production, power engineering and food engineering. Many of the non-Newtonian fluids used in chemical engineering follow the empirical Ostwald–de Waele power-law model for the shear stress. Char and Chen [19] considered the flow and heat transfer of such a fluid over a stretching surface with variable heat flux condition at the wall. Pop et al. [20] studied the heat transfer characteristic of a non-Newtonian fluid over a moving cylinder. Pop and Gorla [21] obtained the second-order boundary layer solution for this problem. Tsai and Hsu [22] investigated the conjugate convection–conduction heat transfer of a non-Newtonian power-law fluid over a continuously moving plate and obtained the solution of the governing boundary layer equations by using cubic spline collocation method.

This paper considers the conjugate heat transfer problem including convection and conduction from a heated vertical plate of finite thickness moving with a constant velocity in a non-Newtonian power-law fluid. The buoyancy force arises due to the temperature difference between the heated surface and the fluid. The partial difference equations governing the natural convection flow over a vertical moving surface have been solved numerically by using an implicit finite-difference method [23,24]. The effects of the buoyancy and non-Newtonian parameters, generalized Prandtl number, Peclet number and the parameter characterizing the material properties of the fluid and plate have been examined in details. The results have been compared with those of Karwe and Jaluria [13] and Tsai and Hsu [22]. Our problem may be regarded as an extension of the work of Karwe and Jaluria [13] to include the effects of non-Newtonian fluids and of Tsai and Hsu [22] to include the effects of buoyancy forces. The present

analysis will be useful in wire plastic coating process. In this case, the metal wire is coated with a plastic sheath from an extruder and then the insulated wire passes through a cooling system. The size of the cooling bath varies according to the volume of the plastic to be cooled. The length of the bath can be calculated depending upon properties of the materials, the conditions of extrusion, i.e., speed, temperature etc., and the temperature of the cooling medium. With increasing speeds of extrusion, the amount of time the material spends in the cooling bath can be reduced.

2. Formulation and analysis

Let us consider a continuous vertical heated plate of thickness $2d$ (Fig. 1). The plate emerges from a slot at constant temperature T_0 and is continuously moving with uniform velocity U_0 in an otherwise quiescent non-Newtonian fluid with constant temperature T_∞. The temperature T_0 of the plate is much higher than the fluid temperature T_∞ ($T_0 > T_\infty$) and this gives rise to buoyancy forces. The induced motion of the fluid is assumed to be laminar, steady, and two-dimensional with thermally active incompressible viscous fluid with constant properties. Due to the viscous drag at the surface of the place, flow is induced in the vicinity of the plate surface. The plate also loses energy to the ambient fluid. We take two different stationary axes at the origin located at the slot. The positive x-axis is parallel to the plate and in the direction of the motion of the plate. The y-axis for the fluid is outside the plate and for the plate it is located inside the plate and is denoted by y_p. The two scales originate at the slot and extend normal to the plate. The buoyancy force acts in the negative x direction. Viscous dissipation in the energy equation has been neglected. The non-Newtonian fluid is assumed to follow the Ostwald–de Waele power-law model. Here we have used the boundary layer approximations which are not valid at or near the slot. In addition, the energy equation for the temperature distribution within the moving plate is used, neglecting the axial conduction. Under the above assumptions and invoking the Boussinesq approximation, the boundary layer equations based on the conservation of mass, momentum and energy governing the flow and heat transfer of a non-Newtonian power-law fluid over a moving vertical plate can be expressed as [13,22]

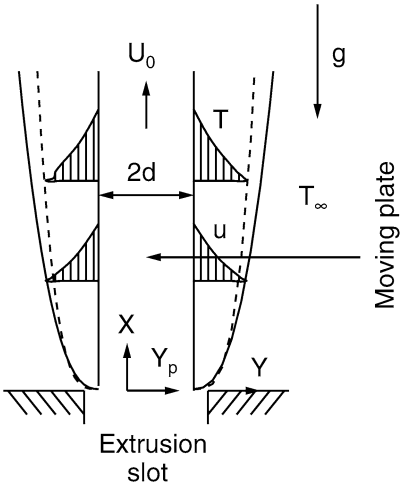

Fig. 1. Physical model and coordinate system.

$$\frac{\partial u}{\partial x} + \frac{\partial v}{\partial y} = 0 \tag{1}$$

$$u\frac{\partial u}{\partial x} + v\frac{\partial u}{\partial y} = \frac{m}{\rho}\frac{\partial}{\partial y}\left[\left|\frac{\partial u}{\partial y}\right|^{N-1}\frac{\partial u}{\partial y}\right] + g\beta(T - T_\infty) \tag{2}$$

$$u\frac{\partial T}{\partial x} + v\frac{\partial T}{\partial y} = \alpha_f\frac{\partial^2 T}{\partial y^2} \tag{3}$$

The boundary conditions for the flow field are given by

$$\begin{aligned} &u = v = 0, \quad T = T_\infty \quad \text{for } x = 0,\ y > 0,\\ &u = U_0, \quad v = 0, \quad T = T_p(x, d) \quad \text{for } x \geqslant 0,\ y = 0\\ &u \to 0, \quad T \to T_\infty \quad \text{for } x > 0,\ y \to \infty \end{aligned} \tag{4}$$

The energy equation for the temperature distribution within the moving plate neglecting the axial conduction is given by

$$U_0\frac{\partial T_p}{\partial x} = \alpha_p\frac{\partial^2 T_p}{\partial y_p^2} \tag{5}$$

with the corresponding boundary conditions

$$\begin{aligned} &T_p(0, y_p) = T_0 \quad \text{for } x = 0\\ &\frac{\partial T_p}{\partial y_p} = 0 \quad \text{for } x \geqslant 0,\ y_p = 0\\ &K_p\frac{\partial T_p}{\partial y_p} = K_f\left(\frac{\partial T}{\partial y}\right)_{y=0} \quad \text{for } x > 0,\ y_p = d \end{aligned} \tag{6}$$

Here x and y are the distances along and normal to the plate, u and v are the velocity components along x and y directions, N is the index in the power-law variation of the surface shear stress and $N < 1$ for pseudoplastic fluids, $N > 1$ for dilatant fluids and $N = 1$ for Newtonian fluids, T is the temperature, T_0 is the temperature of the plate at the slot, g is the acceleration due to the gravity, ρ is the density, β is the volumetric coefficient of the thermal expansion, m is the consistency of power-law fluids, α is the thermal diffusivity, $2d$ is the thickness of the plate, K is the thermal conductivity, the subscripts f and p denote values in the fluid and at the plate, and the subscripts w and ∞ denote conditions at the wall and in the ambient fluid.

By using the vectorial dimensional analysis of Chida and Katto [25] which distinguishes phases it can be shown that the main factors that affect this problem are three: physical properties of the fluid and plate material, buoyancy force and non-Newtonian parameter. On the other hand, the approach of Karwe and Jaluria [13] and Tsai and Hsu [22] shows that this phenomenon is affected by buoyancy force λ, non-Newtonian parameter N, Prandtl number Pr, Peclet number Pe and physical properties parameter R. Therefore the analysis of Chida and Katto [25] yields more compact representation. However, we have followed the analysis of Karwe and Jaluria [13] and Tsai and Hsu [22] so that our results could directly be compared with their results.

It is convenient to work with dimensionless equations. Hence, we apply the following transformations

$$X = x/L, \qquad Y = y\,Re_L^{1/(1+N)}/L, \qquad Y_p = y_p/d$$
$$U = u/U_0, \qquad V = (v/U_0)Re_L^{1/(N+1)}$$
$$\theta = (T - T_\infty)/(T_0 - T_\infty), \qquad \theta_p = (T_p - T_\infty)/(T_0 - T_\infty)$$
$$Re_L = U_0^{2-N} L^N/(m/\rho)$$
$$Gr_L = g\beta(T_0 - T_\infty)L^3/(\alpha_f Pr)^2$$
$$Pr = U_0 L(Re_L)^{-2/(N+1)}/\alpha_f$$
$$Pe = U_0 d^2/(\alpha_p L), \qquad R = \left[(K\rho c)_f/(K\rho c)_p\right]^{1/2}$$
$$\lambda = Gr_L/(Re_L)^{4/(N+1)} = g\beta(T_0 - T_\infty)L/U_0^2 \tag{7}$$

to Eqs. (1)–(6) and we get the following system of equations.

For the fluid

$$\frac{\partial U}{\partial X} + \frac{\partial V}{\partial Y} = 0 \tag{8}$$

$$U\frac{\partial U}{\partial X} + V\frac{\partial U}{\partial Y} = \frac{\partial}{\partial Y}\left[\left|\frac{\partial U}{\partial Y}\right|^{N-1}\frac{\partial U}{\partial Y}\right] + \lambda\theta \tag{9}$$

$$U\frac{\partial \theta}{\partial X} + V\frac{\partial \theta}{\partial Y} = Pr^{-1}\frac{\partial^2 \theta}{\partial Y^2} \tag{10}$$

For conduction within the plate (neglecting the conduction in x-direction)

$$\frac{\partial \theta_p}{\partial X} = Pe^{-1}\frac{\partial^2 \theta_p}{\partial Y_p^2} \tag{11}$$

with boundary conditions for the fluid and plate [22]

$$U = V = \theta = 0, \qquad X = 0, \qquad Y > 0$$
$$U = 1, \qquad V = 0, \qquad \theta = \theta_p(X, 1), \qquad X \geqslant 0, \qquad Y = 0$$
$$U \to 0, \qquad \theta \to 0, \qquad X > 0, \qquad Y \to \infty$$
$$\theta_p(0, Y_p) = 1, \qquad X = 0$$
$$\frac{\partial \theta_p}{\partial Y_p} = 0, \qquad X \geqslant 0, \qquad Y_p = 0$$
$$\frac{\partial \theta_p}{\partial Y_p} = R(Pe/Pr)^{1/2}\left(\frac{\partial \theta}{\partial Y}\right)_{Y=0}, \qquad X > 0, \qquad Y_p = 1 \tag{12}$$

The symbol L used above stands for an arbitrarily chosen length scale in the boundary layer approximation. Since there is no representative length scale along the length of the plate, any arbitrarily chosen value of L may be employed for non-dimensionalization and for yielding results in the entire flow field. This is similar to the self-similar flow over a stationary plate. Here we have taken $L = 0.25$ m.

Here X and Y are the dimensionless distances along and perpendicular to the plate, U and V are the dimensionless velocity components along X and Y directions, θ is the dimensionless temperature, Re_L is the Reynolds number, Gr_L is the Grashof number, Pe is the Peclet number, Pr is the generalized Prandtl number, λ is the buoyancy parameter, R is the physical properties parameter and the subscripts f and p denote fluid and plate, respectively.

It may be noted that Eqs. (8)–(12) for $N = 1$ (Newtonian fluids) are identical to those of Karwe and Jaluria [13] and for $\lambda = 0$ (forced convection flow) with those of Tsai and Hsu [22]. In the absence of conduction within the plate ($\theta_p = 1$) and $N = 1$, Eqs. (8)–(10) are identical to those of Moutsoglou and Chen [8] when $\lambda \geqslant 0$ and to those of Tsou et al. [4], Erickson et al. [5] and Griffin and Thorne [6] when $\lambda = 0$.

The quantities of physical interest are the local Nusselt number Nu_x and skin friction coefficient C_{fx} and they are expressed as

$$Nu_x = -L(\partial T/\partial y)_{y=0}/(T_0 - T_\infty)$$
$$= -(Re_L)^{1/(N+1)}(\partial\theta/\partial Y)_{Y=0}$$
$$C_{fx} = m\left(|\partial u/\partial y|\right)_{y=0}^N/\rho U_0^2$$
$$= (Re_L)^{-1/(N+1)}\left(\frac{\partial U}{\partial Y}\right)_{Y=0}^N \tag{13}$$

where Nu_x and C_{fx} are the local Nusselt number and skin friction coefficient, respectively.

It may be remarked that the results in the elliptic region close to the slot obtained by using the boundary layer approximations would be unrealistic. The accuracy of such results near the slot can be determined by comparison of elliptic solutions (Navier–Stoker equations) and parabolic solutions (boundary layer equations). However, some useful information about the value of the distance X beyond which the boundary layer approximations are valid can be obtained by linking the values of X $(= x/L)$ to the values of Reynolds number $Re_x (= U_0^{2-N} x^N/(m/\rho))$ and Richardson number $Ri_x (= g\beta(T_0 - T_\infty)x/U_0^2)$ based on the distance x measured from the slot along the plate provided L is known [18]. Since L is an arbitrarily chosen length scale, it is not possible to obtain the value of X beyond which the boundary layer approximations are valid.

3. Method of solution

Eqs. (8)–(11) under conditions (12) have been solved by using an implicit tri-diagonal variable step size finite-difference methodology similar to that discussed by Blottner [23] and Patankar [24]. Variable step size in X and Y directions has been used. The initial step size and the growth factor in Y and X directions are 0.001, 1.03, and 0.01, 1.01, respectively. All first-order derivatives with respect to X are replaced by two-point backward difference formulae. Eqs. (9), (10) and (12) are discretized by using three-point central difference formulae in Y direction, whereas in Eq. (8) the first order derivative with respect to Y is discretized by using trapezoidal rule. The problem is solved as an initial value problem with X playing the role of time. At each line of constant X, linear tri-diagonal matrix of linear algebraic equations has been solved by using the Thomas algorithms [23] where iteration has been used to deal with the nonlinear terms in the governing equations. A convergence criterion based on the difference between the current and previous iterations is used. If this difference reaches 10^{-5}, the solution is assumed to have converged and the iterative process is terminated. The choice of initial step size and the growth factors in X and Y directions has been arrived after numerical experimentation to ensure grid independence.

4. Results and discussion

As mentioned earlier, we have solved the governing equations by using an implicit finite-difference scheme. For Newtonian fluids ($N = 1$) in the absence of conduction within the plate ($\theta_p = 1$), we have compared the velocity profile (u/U_0) for $\lambda = 0$, $X = 3$ with the theoretical and experimental results of Tsou et al. [4]. The comparison is shown in Fig. 2. The velocity profile is found to be in very good agreement with the theoretical results. It also agrees well with the experimental results near the wall. Further the Nusselt number Nu_x for $\lambda = 0$, $X = 3$ has been compared with the theoretical values of Erickson et al. [5] and experimental values of Griffin and Thorne [6]. The comparison is presented in Fig. 3. The results are in good agreement with the theoretical and experimental values when the wall velocity $U_0 > 8.96(ft/s)$. We have also compared the surface shear stress ($\partial U(X,0)/\partial Y$) and the surface heat transfer ($-\partial\theta(X,0)/\partial Y$) for $\theta_p = 1$, $X = 3$ with the tabulated results of Moutsoglou and Chen [8]. The results are found to be in very good agreement. The maximum difference is found to be about 1%. Hence the comparison is not shown here. The results for $X \geqslant 3$ correspond to self-similar flow. Hence the results for $X > 3$ can also be used. Further, we have compared the variation of the centerline temperature θ_c with X for $R = 1.092$, $N = 1$, $Pr = 7$, $\lambda = 0$, $Pe = 0.01, 0.1, 1.0$ with that of Karwe and Jaluria [13]. We have also compared the Nusselt number ($Re_L^{-1/(N+1)}\theta_w Nu_x$) for $\lambda = 0$, $N = R = 0.5$, $Pe = 0.1$, $Pr = 10, 50, 100$ with that of Tsai and Hsu [22]. In

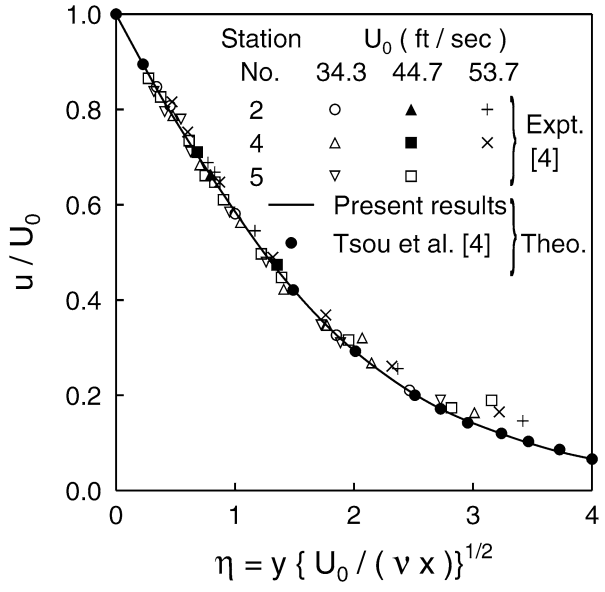

Fig. 2. Comparison of the velocity profile u/U_0 for $\lambda = 0$, $N = 1$, $X = 3$ with that of Tsou et al. [4].

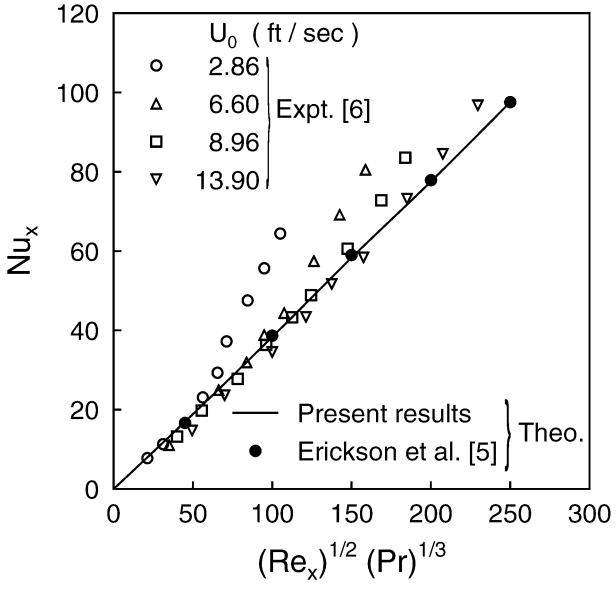

Fig. 3. Comparison of the local Nusselt number Nu_X for $\lambda = 0$, $N = 1$, $X = 3$ with that of Erickson et al. [5], and Griffin and Thorne [6].

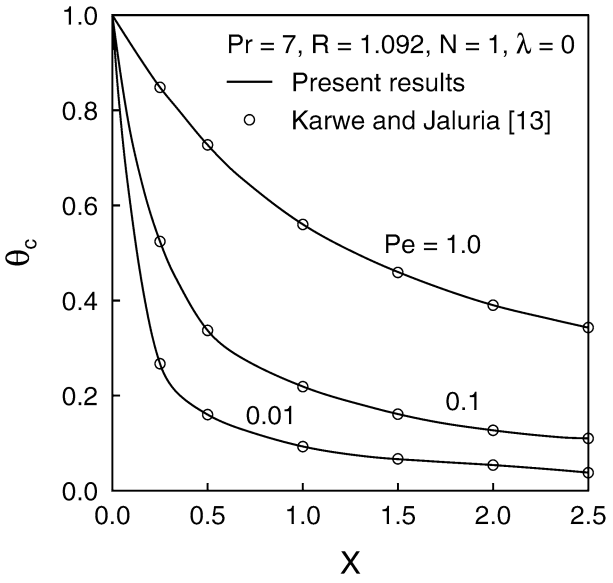

Fig. 4. Comparison of the centerline temperature, θ_c, for $N = 1$ with that of Karwe and Jaluria [13].

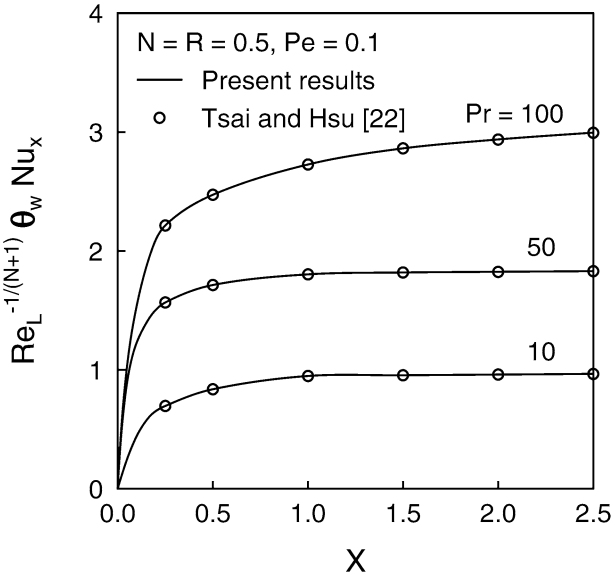

Fig. 5. Comparison of the local Nusselt number, $Re_L^{-1/(N+1)}\theta_w Nu_x$, with that of Tsai and Hsu [22].

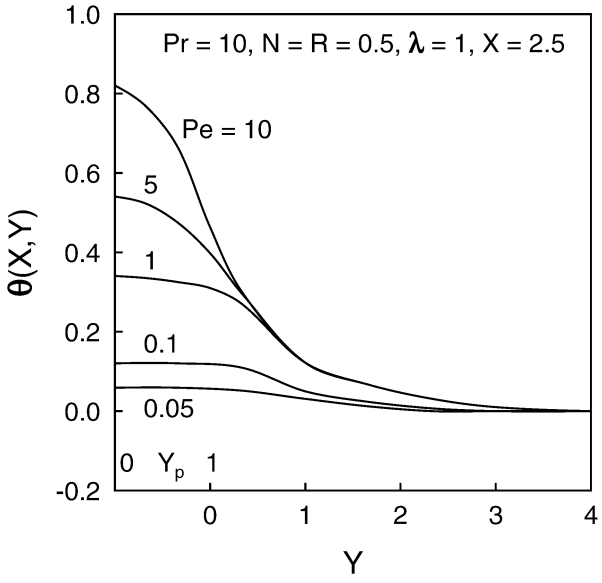

Fig. 6. Effects of the Peclet number Pe on the temperature distribution along the transverse direction Y, $\theta(X, Y)$.

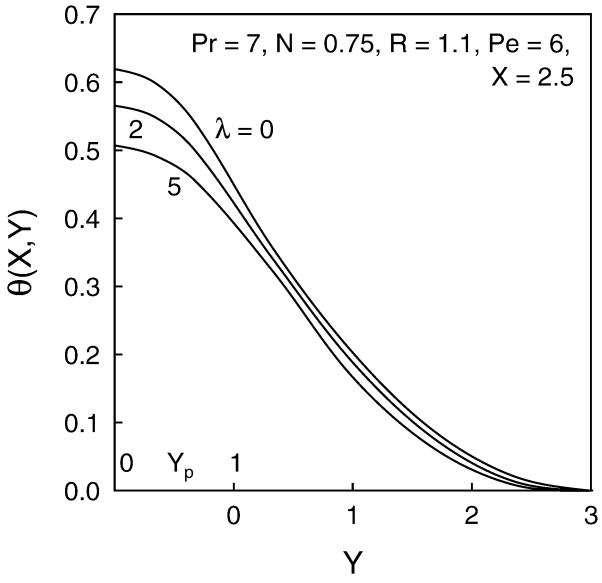

Fig. 7. Effects of the buoyancy parameter λ on the temperature distribution along the transverse direction Y, $\theta(X, Y)$.

both cases, the results are in very good agreement. The comparison is shown in Figs. 4 and 5.

The distribution of temperature θ along the transverse direction Y for several values of Pe when $Pr = 10, \lambda = 1, R = N = 0.5, X = 2.5$ is shown in Fig. 6. It is evident from Fig. 6 that the temperature profiles in the Y direction are nearly uniform within the plate for small Pe. Therefore, the assumption of uniform temperature across the plate is justified in the governing equation for the plate. The information on the temperature distribution is useful for the design of system required for the particular manufacturing process.

Fig. 7 shows the effect of λ on the temperature profiles $\theta(X, Y)$. θ decreases with increasing λ due to the reduction in the thermal boundary layer thickness.

Fig. 8 displays the effects of the buoyancy parameter λ on the local Nusselt number ($Re_L^{-1/(N+1)} Nu_x$) and the surface temperature (θ_w) for $N = R = 0.5, Pr = 10, Pe = 0.1$. Since the positive buoyancy force ($\lambda > 0$) acts like a favourable pressure gradient, the fluid is accelerated which results in thinner momentum and thermal boundary layers. Consequently, the Nusselt number and wall temperature increase with λ. Since the wall temperature tends to the ambient temperature away from the slot, it continuously decreases with the distance X. Hence the Nusselt number also decreases with the increasing distance X. The above results are important in determining the effects of the buoyancy forces on the thermal transport. They are also useful in the determination of the length of the system. For fixed values of other parameters, a simple correlation equation for the local Nusselt number Nu_x which is valid (within 5% error) for $0 \leqslant \lambda \leqslant 10$, $X > 1.5$ is given by

$$Nu_x/Nu_x^* = 1 + 0.1392\lambda + 0.0012\lambda^2$$

where Nu_x^* is the Nusselt number for $\lambda = 0$.

Fig. 9 presents the effects of the buoyancy parameter λ on the local skin friction coefficient ($Re_L^{1/(N+1)} C_{fx}$) for $N = R =$

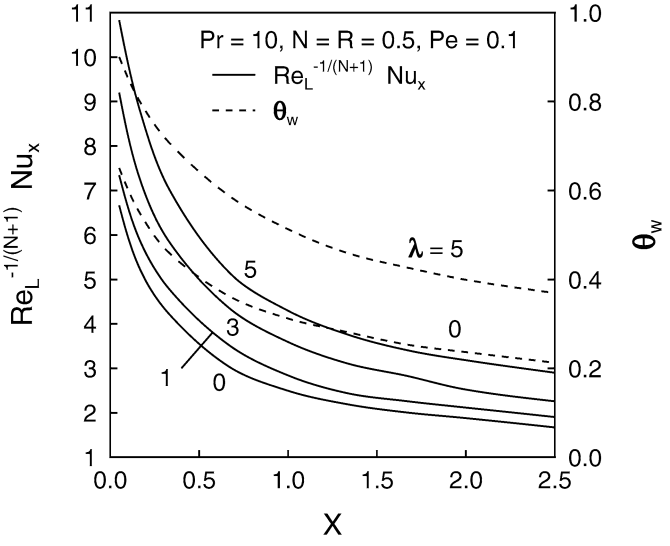

Fig. 8. Effects of the buoyancy parameter λ on the local Nusselt number, $Re_L^{-1/(N+1)} Nu_x$, and wall temperature, θ_w.

$0.5, Pr = 10, Pe = 0.1$. As mentioned earlier, the positive buoyancy force acts like a favourable pressure gradient which accelerates the fluid in the boundary layer. This results in thinner boundary layer and hence in higher velocity gradient at the surface. Therefore, the skin friction coefficient increases with λ. For a fixed λ, the skin friction coefficient decreases with increasing streamwise distance X. The reason for this trend is that the boundary layer grows with the distance X which reduces the fluid motion in the boundary layer. Consequently, the velocity gradient and hence the skin friction coefficient progressively reduce as X increases.

Fig. 10 shows the effect of the non-Newtonian parameter N on the skin friction coefficient ($Re_L^{1/(N+1)} C_{fx}$) for $Pr = 10$, $Pe = 0.1, R = 0.5, \lambda = 3$. The effect of N is found to be more pronounced on the skin friction than on the heat transfer,

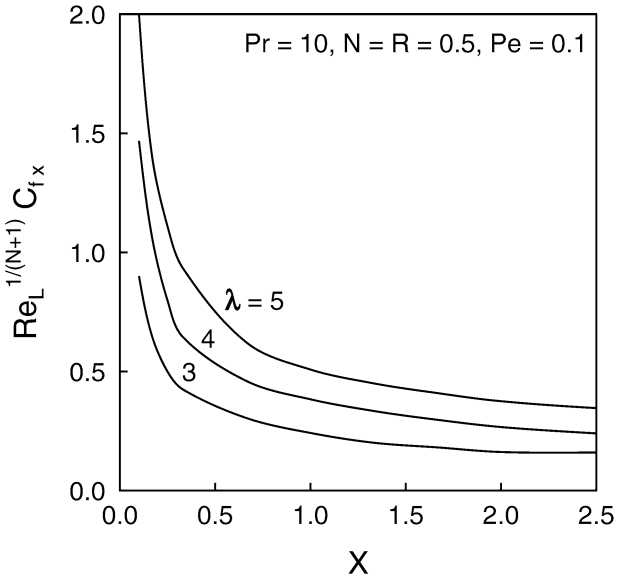

Fig. 9. Effects of the buoyancy parameter λ on the local skin friction coefficient, $Re_L^{1/(N+1)} C_{fx}$.

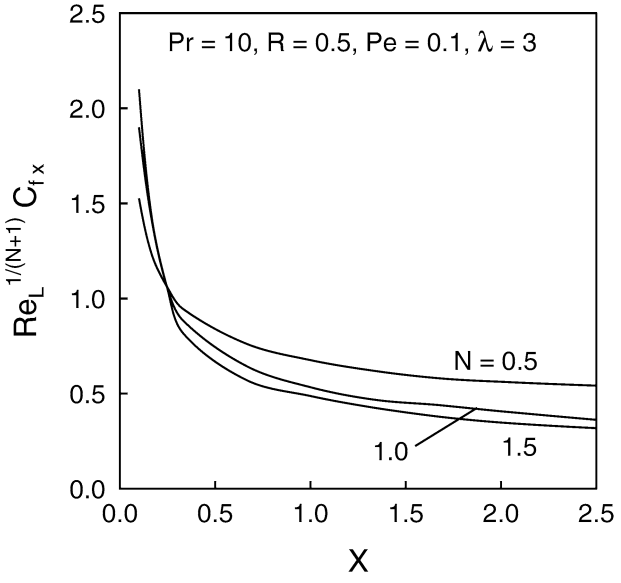

Fig. 10. Effects of the non-Newtonian parameter N on the local skin friction coefficient, $Re_L^{1/(N+1)} C_{fx}$.

since N affects the momentum equation directly. In the region $0.1 \leqslant X < 0.3$, the skin friction coefficient for the dilatant fluid ($N > 1$) is found to be more than that of the pseudoplastic fluid ($N < 1$), and beyond this region it is the other way around. This trend is due to the relative importance of other parameters. For a given fluid medium, the skin friction coefficient decreases with increasing distance X. This behaviour is due to the increase in the boundary layer thickness with X. Consequently, the velocity gradient and hence the skin friction coefficient decrease with increasing X. Like the skin friction coefficient, the Nusselt number also decreases with increasing X. This is due to the reduction in the temperature difference as we move downstream from the slot. As mentioned earlier, the effect of N on the Nusselt number is small. Hence it is not shown here.

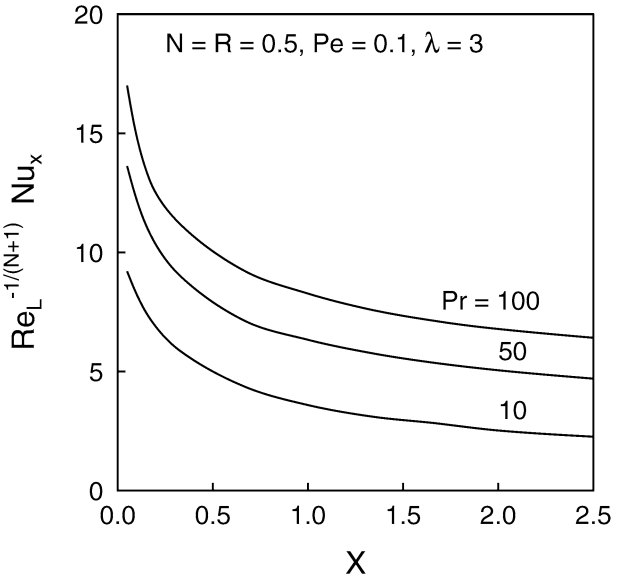

Fig. 11. Effects of the Prandtl number Pr on the local Nusselt number, $Re_L^{-1/(N+1)} Nu_x$.

The effects of the generalized Prandtl number Pr on the local Nusselt number ($Re_L^{-1/(N+1)} Nu_x$) for $\lambda = 3, N = R = 0.5, Pe = 0.1$ are shown in Fig. 11. Since the increase in the Prandtl number Pr results in thinner thermal boundary layer, the Nusselt number increases with Pr. At $X = 2.5$, the Nusselt number increases by about 178% as Pr increases from 10 to 100. For a fixed Pr, the Nusselt number decreases with increasing X. The reason for this trend has been explained earlier. The correlation equation (within 8% difference) can be expressed as

$$Nu_x/Nu_x^* = 1 + 0.0231Pr - 10^{-4} \times 0.53Pr^2$$
$$10 \leqslant Pr \leqslant 200,\ X > 1.5$$

where Nu_x^* is the Nusselt number for $Pr = 10$.

Fig. 12 illustrates the effects of the Peclet number Pe on the surface temperature θ_w and the local Nusselt number ($Re_L^{-1/(N+1)} Nu_x$) for $\lambda = 3, N = R = 0.5, Pr = 10$. The increase in Peclet number Pe implies that the plate is exposed to the cooler ambient fluid for shorter durations. Hence less energy is lost from the surface. Consequently, the surface temperature and the Nusselt number increase with Pe. In this case, the correlation equation (within 10% difference) can be written as

$$Nu_x/Nu_x^* = 1 + 0.23605Pe - 0.02775Pe^2$$
$$0.05 \leqslant Pe \leqslant 5,\ X > 1.5$$

where Nu_x^* is the Nusselt number for $Pe = 0.05$.

Fig. 13 presents the effects of the material parameter R on the surface temperature θ_w and the local Nusselt number ($Re_L^{-1/(N+1)} Nu_x$) for $\lambda = 3,\ N = 0.5,\ Pe = 0.1,\ Pr = 10$. For smaller values of R (i.e., for a plate with large thermal capacity or high thermal conductivity), the Nusselt number and surface temperature are more than those for larger values of R. Hence the heat transfer or surface temperature can be reduced by proper choice of R.

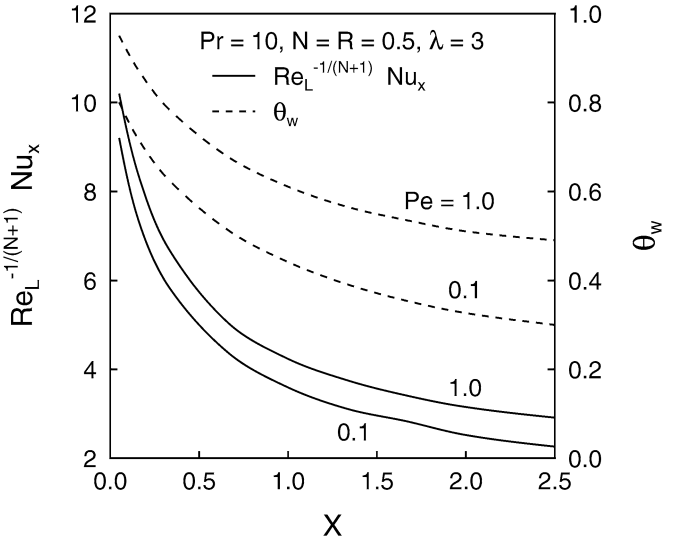

Fig. 12. Effects of the Peclet number Pe on the local Nusselt number, $Re_L^{-1/(N+1)}Nu_x$, and the wall temperature, θ_w.

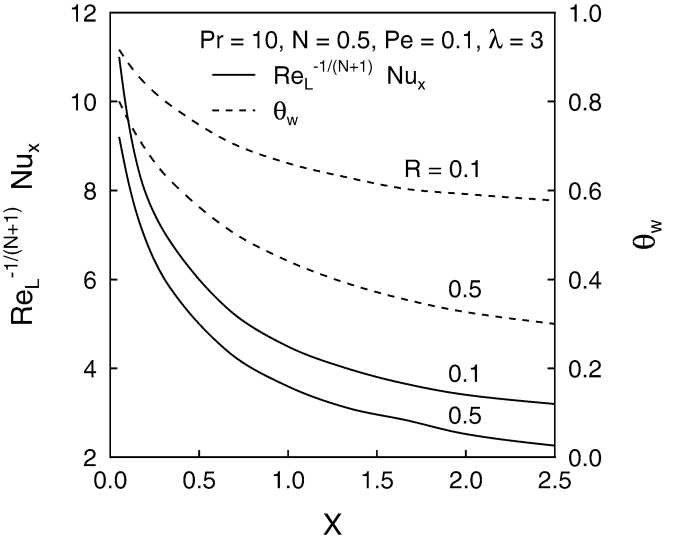

Fig. 13. Effects of R on the local Nusselt number, $Re_L^{-1/(N+1)}Nu_x$, and the wall temperature, θ_w.

5. Conclusions

The heat transfer increases with the buoyancy force, Prandtl number and Peclet number, but it decreases with increasing material parameter. The skin friction and the Nusselt number show some interesting behaviour for the non-Newtonian fluids characterized by the parameter N. They increase with the non-Newtonian parameter near the slot, but show opposite trend away from the slot. The surface temperature and the Nusselt number decay in the material as one moves away from the slot or die. The above results are useful in the evaluation of the relative importance of various parameters in the thermal transport and in determining the system length required for attaining a given temperature level. Also, if there is a limitation on the total length of the system, the present results can be employed to determine if any additional cooling arrangement is needed or if the choice of the fluid will be required. Any practical system has to consider all these factors in achieving the optimized design.

References

[1] T. Altan, S. Oh, H. Gegel, Metal Forming Fundamentals and Applications, American Society of Metals, Metals Park, OH, 1970.
[2] E.G. Fisher, Extrusion of Plastics, Wiley, New York, 1976.
[3] B.C. Sakiadis, Boundary layer behaviour on continuous solid surface, II. The boundary layer on a continuous flat surface, AIChE J. 7 (1961) 221–225.
[4] F.K. Tsou, E.M. Sparrow, K.J. Goldstein, Flow and heat transfer in the boundary layer on a continuous moving surface, Int. J. Heat Mass Transfer 10 (1967) 219–235.
[5] L.E. Erickson, L.T. Fan, V.G. Fox, Heat and mass transfer on a moving continuous flat plate with suction or blowing, Ind. Engrg. Chem. Fund. 5 (1966) 19–25.
[6] J.F. Griffin, J.L. Thorne, On the thermal boundary layer growth on continuous moving belts, AIChE J. 13 (1967) 1210–1211.
[7] D.R. Jeng, T.C.A. Chang, K.J. DeWitt, Momentum and heat transfer on a continuous moving surface, J. Heat Transfer 108 (1986) 532–537.
[8] A. Moutsoglou, T.S. Chen, Buoyancy effects in boundary layers on inclined continuous moving sheets, J. Heat Transfer 102 (1980) 171–173.
[9] H.S. Takhar, A.J. Chamkha, G. Nath, Effect of buoyancy forces on the flow and heat transfer over a continuous moving vertical or inclined surface, Int. J. Thermal Sci. 40 (2001) 825–833.
[10] Y. Jaluria, A.P. Singh, Temperature distribution in a moving material subjected to surface energy transfer, Comput. Math. Appl. Mech. Engrg. 41 (1983) 145–157.
[11] K. Chida, Y. Katto, Conjugate heat transfer of continuously moving surfaces, Int. J. Heat Mass Transfer 19 (1976) 461–470.
[12] M.V. Karwe, Y. Jaluria, Thermal transport from heated moving surface, J. Heat Transfer 108 (1986) 728–733.
[13] M.V. Karwe, Y. Jaluria, Fluid flow and mixed convection transport from a moving plate in rolling and extrusion processes, J. Heat Transfer 110 (1988) 655–661.
[14] M.V. Karwe, Y. Jaluria, Numerical simulation of thermal transport associated with a continuously moving flat sheet in materials processing, J. Heat Transfer 113 (1991) 612–619.
[15] B.H. Kang, Y. Jaluria, Heat transfer from continuously moving material in channel flow for thermal processing, J. Thermophys. Heat Transfer 8 (1994) 546–554.
[16] R. Viskanta, T.L. Bergman, Heat transfer in materials processing, in: W.M. Rohsenow, J.P. Hartnett, Y.I. Cho (Eds.), Handbook of Heat Transfer, third ed., McGraw-Hill, New York, 1998, pp. 18.1–18.74 (Chapter 18).
[17] S.A. Al-Sanea, M.E. Ali, The effect of extrusion slit on the flow and heat transfer characteristics from a continuously moving material with suction or injection, Int. J. Heat Fluid Flow 21 (2000) 84–91.
[18] S.A. Al-Sanea, Convection regimes and heat transfer characteristics along a continuously moving heated vertical plate, Int. J. Heat Fluid Flow 24 (2003) 888–901.
[19] M.I. Char, C.K. Chen, Temperature field in non-Newtonian flow over a stretching plate with variable heat flux, Int. J. Heat Mass Transfer 81 (1988) 917–921.
[20] I. Pop, M. Kumari, G. Nath, Non-Newtonian boundary layer on a moving cyclinder, Int. J. Engrg. Sci. 28 (1990) 303–312.
[21] I. Pop, R.S.R. Gorla, Second-order boundary layer solution for a continuous moving surface in a non-Newtonian fluid, Int. J. Engrg. Sci. 28 (1990) 313–322.
[22] S.Y. Tsai, T.H. Hsu, Thermal transport of a continuous moving plate in a non-Newtonian fluid, Comput. Math. Appl. 29 (1995) 99–108.
[23] F.G. Blottner, Finite-difference methods of solution of the boundary layer equations, AIAA J. 8 (1970) 193–205.
[24] S.V. Patankar, Numerical Heat Transfer and Fluid Flow, McGraw-Hill, New York, 1980.
[25] K. Chida, Y. Katto, Study on conjugate heat transfer by vectorial dimensional analysis, Int. J. Heat Mass Transfer 19 (1976) 453–460.